Two-level systems and low-temperature glass dynamics: Spectral diffusion and thermal reversibility of hole-burning linewidths

K. A. Littau, Y. S. Bai, and M. D. Fayer
Department of Chemistry, Stanford University, Stanford, California 94305

(Received 2 November 1989; accepted 28 December 1989)

Intermediate time-scale time-dependent hole-burning measurements are reported on three glassy organic systems which undergo spectral diffusion: cresyl violet in ethanol at 1.30 and 2.13 K, resorufin in ethanol at 2.13 K, and resorufin in glycerol at 2.13 K. The hole width is observed to broaden on a log time scale from 0.1 to 5000 s for each ethanol system while no broadening is observed in the system of resorufin in glycerol. A detailed theoretical treatment is introduced which allows the raw data to be converted to the fluctuation rate distribution of the underlying modes responsible for dephasing. Using this theory, the broadening in ethanol is found to be the result of a distribution of glassy modes which is Gaussian on a log R scale with a center rate at $\sim 0.02\ s^{-1}$. In addition, temperature cycling hole-burning results are reported on the system cresyl violet in ethanol. A hole is burned at 1.30 K and detected before, during, and after a temperature cycle to 2.13 K and back. The hole width is observed to broaden at the high temperature and then narrow again in a completely reversible manner when the temperature is again lowered. Theoretical calculations show this behavior to be entirely consistent with the tunneling two-level-system (TLS) model of glass dynamics but incompatible with other models such as particle or defect diffusion. The cycling data is shown to fall exactly on the theoretical curve calculated from the TLS model using no adjustable parameters.

I. INTRODUCTION

The dynamics of low-temperature glasses have been and continue to be the subject of a great deal of experimental and theoretical study.[1-9] Over twenty years ago glasses were recognized to be fundamentally different from crystals. When applied to glasses, models used to explain crystal thermodynamics deviated from experiment at low temperatures.[5] Observation of such phenomena as time-dependent[6,7] and anomalously high heat capacities[5] illustrate some of the differences. Because glasses are nonequilibrium structures, they have many different microscopic configurations which are nearly equivalent in energy—quite unlike the single sharp global potential surface minimum associated with a crystal structure. These nearly equivalent states have been used to account for the increased density of low-energy modes responsible for the large low-temperature heat capacities. Because of the disordered nature of glasses, these low-energy modes have a wide distribution of relaxation rates. Thus, even at low temperature, a glass is still a dynamic system exhibiting dynamics over many orders of magnitude in time—from picoseconds to kiloseconds or longer.[1]

Anderson, Halperin, and Varma[8] and Phillips[9] independently proposed models for low-temperature glasses which described the dynamics as localized low-frequency modes—two-level systems (TLS's). A TLS involves an asymmetric double potential well. Transitions between the two wells represent changes in the local structure of the glass. Since its introduction, the TLS model has had great success in describing a variety of low-temperature glassy properties including anomalous heat capacities,[5] ultrasonic attenuation,[10-12] phonon echoes,[13] photon echoes,[14-17] and hole burning.[18] However, while it does well in modeling the dynamics, the TLS theory, as was recently pointed out,[19] is still only one of several possible explanations of these properties. Models consisting of particle diffusion and multilevel structures could also, in theory, be used with equal success.[19,20] Some papers[18] have commonly been referred to as demonstrations of the validity of the TLS model; however, while these references clearly demonstrate the success of the theory, they are not proofs that the model is, in fact, valid. In this paper the results of several waiting-time-dependent hole-burning experiments and calculations are presented which clarify the quesion of whether the TLS model is an accurate physical description of the microscopic nature of low-temperature glasses.

Two facets of persistent spectral hole burning are used to examine the characteristics of glass dynamics. First, using a variable waiting-time experiment described in Sec. III, it is shown that the glasses under study have a distribution of fluctuation rates across several orders of magnitude in time. Second, using a temperature-cycling experiment also described in Sec. III, it is demonstrated that the dynamics responsible for optical dephasing are caused by a small number of the glass's degrees of freedom while the vast majority of the glass's degrees of freedom are fixed on a time scale well beyond that of the experiment. The static degrees of freedom define many local potential surfaces—each surface corresponding to a single TLS. These potential surfaces are said to be fixed. That is, when the temperature is raised, the potential surfaces do not change. Thus, when the temperature is lowered again, the glass structure returns to the same steady-state configuration it occupied before the temperature cycle. This is in direct contradiction to a diffusion-based model which should show no reversible behavior. In a diffusion-

 0021-9606/90/074145-14$03.00

based model, there are no fixed potential surfaces. Instead, one must consider the N-dimensional potential surface of the entire glass. The glass structure moves randomly on this potential surface. Raising the temperature increases the range and rate of motion. Lowering the temperature again slows this motion but does not reverse its direction.

Persistent spectral hole burning, like photon echoes and other line-narrowing techniques, has been a useful tool in the study of dynamic interactions especially glass dynamics (see, for example, Ref. 4). Recently, however, its usefulness has increased in light of the recognition that hole burning is a "waiting-time-dependent" experiment; hole burning is sensitive to dynamics faster than or on the order of the waiting time between creating and detecting the hole. The first evidence for this came in 1984 when Breinl, Friedrich, and Haarer[21] confirmed the hypothesis that, like other phenomena, the persistent spectral hole width of dye molecules in glasses can be time dependent, that is, it undergoes "spectral diffusion." Spectral diffusion, in this context, means any time-dependent line broadening. A change in hole width of $\sim 30\%$ was reported when the waiting time between burning and detecting the hole was varied from tens of minutes to many days. Broer *et al.*[16] examined stimulated echo and two-pulse echo data and also reported evidence of spectral diffusion. Later, Berg *et al.*[22] compared persistent spectral hole-burning data to two-pulse photon-echo data taken on the same sample and observed a dramatic difference in the dephasing rates measured by the two techniques. The linewidth measured by hole burning was observed to be a factor of 6 greater than the echo-determined linewidth. This was explained in terms of a waiting-time argument. A two-pulse echo experiment is sensitive to fluctuations occurring at times on the order of the pulse separation (typically ps to ns). Hole burning, on the other hand, is sensitive to fluctuations occurring on a time scale from picoseconds out to the waiting time (usually hundreds of seconds). The broader time scale means that there are an increased number of dynamic modes (slow fluctuations) contributing to the hole-burning linewidth. This spectral diffusion leads to a broadening of the hole linewidth.

Temperature-cycling hole-burning experiments have also been of use in examining the properties of glass dynamics. The first such experiment was conducted by Friedrich and Haarer in 1984.[23] Since then it has been used to investigate the irreversible spectral diffusion processes of amorphous materials which appear when the samples are cycled to relatively high temperatures.[24,25] However, when the temperatures are kept low, it is possible to examine the reversible aspects of the dynamics. It is this reversibility and its agreement with theoretical predictions presented here which demonstrate that the glass dynamics occur on fixed local potential surfaces which do not change during the time scale of the experiment.

Recent theoretical work of Bai and Fayer has yielded a powerful tool in the analysis of waiting-time-dependent experiments.[26] It was shown that by analyzing the results of such experiments, it is possible to determine the underlying fluctuation-rate distribution of the sample in question. The fluctuation-rate distribution is the function describing the intrinsic rates and densities of the various dynamic processes responsible for optical dephasing (line broadening). A precise mathematical definition for the fluctuation-rate distribution is given in Sec. II. Key elements of the theory from Ref. 26 are recapitulated in Sec. II as needed to describe the experimental results presented here. After describing and reporting the results of several waiting-time-dependent experiments in Secs. III and IV, Sec. V derives the theory for temperature-cycling hole-burning experiments and compares theory to experiment without recourse to adjustable parameters. The agreement between theory and experiment is excellent and confirms the TLS fixed local potential surface model for glasses.

II. THEORY OF TUNNELING TLS-INDUCED OPTICAL DEPHASING

The TLS theory is very successful in modeling the various aspects of low-temperature glass dynamics.[4,8,9,18,22,26] The TLS model describes fluctuations as discrete jumps between potential minima. These fluctuations are responsbile for optical dephasing in low-temperature glasses. Other models, e.g., defect diffusion, will be discussed in connection to the temperature-cycling experiments. The following analysis is based upon the TLS model.

It has been shown previously that all currently employed line-narrowing techniques used to probe solid-state dynamics, such as photon echoes and hole burning, are theoretically represented by a four-point transition dipole correlation function.[22,27] The general form of the correlation function is[22,28]

$$C(\tau,T_w,\tau) = \langle \mu^*(T_w+2\tau)\mu(T_w+\tau)\mu(\tau)\mu^*(0)\rangle = \left\langle \exp\left[-i\int_0^{\tau}\Delta(t)\,dt + i\int_{T_w+\tau}^{T_w+2\tau}\Delta(t)\,dt \right]\right\rangle , \tag{2.1}$$

where τ, T_w, and τ are the intervals between the four times in the correlation function, and $\Delta(t)$ is the time-dependent perturbation of the transition frequency. Equation (2.1) is the function which describes the decay of the stimulated photon echo—in a sense, the most general of the line-narrowing experiments. In this context, τ represents the delay between the first two pulses of the stimulated-echo pulse sequence, while T_w is the delay between the second and third pulses. The echo then occurs τ after the third pulse. It has been shown that the correlation functions describing the results of the other line-narrowing experiments may be derived from Eq. (2.1).[22,26,28] For example, the spectrum of a hole generated in a hole-burning experiment is the Fourier transform of the stimulated-echo correlation function.[22] That is,

$$I_H(\omega_R-\omega_B) \propto \int d\tau \exp[i(\omega_R-\omega_B)\tau]C(\tau,T_w,\tau) , \tag{2.2}$$

where ω_R and ω_B are the reading and burning laser frequencies, respectively, and T_w is now essentially the waiting time between burning and reading the hole.[29] Note that Eqs. (2.1) and (2.2) predict, in general, a waiting-time (T_w) dependent observable. The correlation function is independent

of T_w only when all the fluctuations are fast relative to τ. Only in this case is the four-point correlation function equivalent to the two-point dipole correlation function of standard line-shape theory.[28,30]

The problem of finding the line shape now becomes one of calculating the four-point correlation function, $C(\tau,T_w,\tau)$. It has been shown[31] that for a large number of independent TLS, Eq. (2.1) can be represented as

$$C(\tau,T_w,\tau)=\exp\{-N\langle 1-\exp[i\phi(\tau,T_w)]\rangle_{H,r,\lambda}\}, \quad (2.3)$$

where $\langle\ \rangle_{H,r,\lambda}$ denotes an average over the random histories, positions, and internal parameters of the perturbing TLS. Here, $\phi(\tau,T_w)$ is the correlation function of a single TLS,

$$\phi(\tau,T_w)=\int_0^{\tau}\Delta\omega(t)\,dt-\int_{T_w+\tau}^{T_w+2\tau}\Delta\omega(t)\,dt, \quad (2.4)$$

where $\Delta\omega(t)$ is the frequency perturbation of the optical center caused by a single TLS. The TLS model assumes that each TLS perturbs the transition of a chromophore by $\pm\Delta\omega$ depending on which level the TLS occupies. That is to say, $\Delta\omega(t)=\pm\Delta\omega$ depending on the level occupation of the TLS. The magnitude of $\Delta\omega$ depends on the distance of the TLS from the chromophore and on the coupling strength.

If the distributions of internal parameters of the TLS are known, the averages in Eq. (2.3) can be carried out. However, in the absence of detailed knowledge of the TLS parameters, Eq. (2.3) may still be solved, and the final solution will be a function of the internal parameter distributions. By comparing to experimental results, one can obtain information about the internal parameter distributions. The remainder of this section is devoted to the reduction of Eq. (2.3) to a form dependent only on the fluctuation-rate distribution by performing the averages in Eq. (2.3).

The history average in Eq. (2.3) has been examined in detail.[26,31,32] In the context of T_w dependent hole burning, it is more informative to analyze Eq. (2.3) only in the long-waiting-time limit, i.e., $T_w\gg\tau$, the situation applicable to all hole-burning experiments.

In the long-time limit, the history average may be calculated using a simple rate-equation description as follows.[26] The rate equations describing the sudden jumps of a single TLS are

$$\frac{d\rho_+}{dt}=-\rho_+R_-+\rho_-R_+,$$
$$\frac{d\rho_-}{dt}=\rho_+R_-+\rho_-R_+, \quad (2.5)$$

where ρ_+ (ρ_-) is the population density of the upper (lower) state, and R_+ (R_-) is the up (down) transition rate. These equations are easily solved to give

$$\Delta\rho(t)-\Delta\rho(\mathrm{eq})=[\Delta\rho(0)-\Delta\rho(\mathrm{eq})]\exp(-Rt),$$
$$\Delta\rho=\rho_+-\rho_-,\quad R=R_++R_-, \quad (2.6)$$

where $\Delta\rho(\mathrm{eq})$ is the population density difference at equilibrium. R is the relaxation rate toward equilibrium.[33]

In the long T_w limit ($\tau\ll T_w,1/R$) the TLS does not flip in a time τ. The accumulated phase error, ϕ, in Eq. (2.4) is then dependent only on the relative state of the TLS at times $t=0$ and $t=T_w$. If the TLS is in the same state at these two times (either never left or has returned), the two integrals in Eq. (2.4) are identical, and the phase error is zero. This leaves only two possible history paths which can give a nonzero phase error. If the TLS is in its upper state at time $t=0$ and the lower state at time $t=T_w$, $\phi=2\Delta\omega t$. Conversely, if the TLS was originally in its lower state and is in its upper state at time $t=T_w$, $\phi=-2\Delta\omega t$.

Using Eq. (2.6), it is possible to find the probability of each of these history paths. Defining p_{+-} to be the probability that the TLS is in the upper state at $t=0$ and the lower state at $t=T_w$, one finds

$$p_{+-}=\rho_+(0)\rho_-[T_w|\rho_+(0)=1]$$
$$=\rho_+(\mathrm{eq})\rho_-(\mathrm{eq})[1-\exp(-RT_w)], \quad (2.7)$$
$$p_{-+}=p_{+-},$$

where $\rho_+(0)$ is the population density of the upper state of the TLS at $t=0$, and $\rho_-[T_w|\rho_+(0)=1]$ is the conditional probability of finding the TLS in its lower state at time $t=T_w$ given it was in its upper state at $t=0$. $\rho_+(\mathrm{eq})$ and $\rho_-(\mathrm{eq})$ indicate the relative population densities at equilibrium. The probabilities that the TLS do not change, p_{++} and p_{--}, may also be calculated, but these situations induce no phase error. With the result of Eq. (2.7), the history average in Eq. (2.3) is calculated to be

$$\langle 1-\exp(i\phi)\rangle_H=p_{+-}[1-\exp(2i\Delta\omega\tau)]$$
$$+p_{-+}[1-\exp(-2i\Delta\omega\tau)]$$
$$=\mathrm{sech}^2(E/2kT)\sin^2(\Delta\omega\tau)$$
$$\times[1-\exp(-RT_w)], \quad (2.8)$$

where E is the TLS energy splitting. Analysis of this function shows it to be an excellent approximation for $1/R,T_w>10\tau$.[26] From this and Eq. (2.3) the correlation function in the long-time limit is found to be

$$C(\tau,T_w,\tau)=\exp\{-N\langle\mathrm{sech}^2(E/2kT)\sin^2(\Delta\omega\tau)$$
$$\times[1-\exp(-RT_w)]\rangle_{r,\lambda}\}. \quad (2.9)$$

Since the distribution of TLS parameters is unknown, the averages in Eq. (2.9) cannot be carried out. Therefore, it is important to express the correlation function in *terms* of the distributions. The average over λ will be performed using an integral over R, the relaxation rate. R is related to the internal parameters of interest according to

$$R=KE\coth(E/2kT)e^{-2\lambda}, \quad (2.10)$$

where K is a collection of constants describing the coupling of the TLS to the glass acoustic phonons, E is again the TLS energy splitting, and λ is the tunneling parameter between the two wells of the TLS.[33] λ is related to the TLS internal parameters according to $\lambda^2=mVd^2/2\hbar^2$, where V is the height of the barrier and d is the distance between the two wells. It is important to note (especially in the context of Sec. V) that R for a particular TLS is, at most, linear in temperature, becoming independent of temperature when $E\gg kT$. Since the distribution of relaxation rates in a glass spans many orders of magnitude in time,[25] a large change in R (approximately an order of magnitude) is required before a significant change in the experimental results can be ob-

served. Thus R is said to be weakly dependent on temperature, weakly meaning that the temperature must change at least one order of magnitude before a change in the distribution of relaxation rates can be observed. When the temperature is raised, as in a temperature dependence or cycling experiment, the fluctuation-rate distribution will shift only slightly. This is in contrast to a thermal hopping process in which the rate is exponentially related to temperature.[25]

The averages in Eq. (2.9) are represented in integral form as

$$\langle \mathrm{sech}^2(E/2kT)\sin^2(\Delta\omega\tau)[1-\exp(-RT_w)]\rangle_{r,\lambda} = \int d\mathbf{r}\, dE\, dR\, P(\mathbf{r},E,R)\mathrm{sech}^2(E/2kT)\sin^2(\Delta\omega\tau) \times [1-\exp(-RT_w)], \quad (2.11)$$

where $P(\mathbf{r},E,R)$ is the normalized probability density of finding a TLS at a position $\mathbf{r}$ (relative to the optical center) with an energy splitting E and relaxation rate R. In general, it is assumed that there is no correlation between position and the internal parameters of the TLS in a glass (however, see Refs. 26 and 34). The following treatment can easily be done making no such assumption.[26,34] In the absence of correlation, $P(\mathbf{r},E,R) = P(\mathbf{r})P(E,R)$, and the integrals may be separated. This leaves

$$\langle \mathrm{sech}^2(E/2kT)\sin^2(\Delta\omega\tau)[1-\exp(-RT_w)]\rangle_{r,\lambda} = f(\tau)\int dE\, dR\, P(E,R)\mathrm{sech}^2(E/2kT) \times [1-\exp(-RT_w)], \quad (2.12)$$

where $f(\tau)$ is the result of the integration over $\mathbf{r}$. $f(\tau)$ contains the information responsible for the line shape (form of the decay) in a hole-burning (photon-echo) experiment.

$P(E,R)$ includes the density of TLS's that are inactive because their energy splittings are much larger than kT; that is, they are not thermally activated. Therefore, we will define a new function, $P(R)$, called the *fluctuation-rate-distribution* function. It is defined to be

$$P(R) = A\int dE\, P(E,R)\mathrm{sec}^2(E/2kT), \quad (2.13)$$

where A is a normalization factor. This function is carefully chosen to be the traditional probability density of TLS, $P(E,R)$, weighted to the degree that each TLS is thermally accessible, or equivalently, it is the rate distribution of the *fluctuating* TLS at a given temperature. It is this function, not $P(E,R)$, which is directly responsible for line broadening. Combining Eqs. (2.12) and (2.13), one obtains

$$\langle \mathrm{sech}^2(E/2kT)\sin^2(\Delta\omega\tau)[1-\exp(-RT_w)]\rangle_{r,\lambda} \propto \int dR\, P(R)[1-\exp(-RT_w)]. \quad (2.14)$$

When the line shape is Lorentzian (echo decay is an exponential), it can be shown that the linewidth is directly proportional to the expression in Eq. (2.14), i.e.,

$$\Delta\omega_H \propto \int dR\, P(R)[1-\exp(-RT_w)], \quad (2.15)$$

where the constant of proportionality is a combination of temperature-independent constants such as the coupling strength of the TLS–chromophore interaction. The line shape is Lorentzian for dipole–dipole coupling between the TLS and the optical center in three-dimensional systems.[22,26,31,35,36] All experimentally measured hole line shapes (echo decays) that have been reported for bulk materials are Lorentzian (exponential).

Equation (2.15) is the final solution in the analysis of a waiting-time-dependent hole-burning experiment. Examining this solution, one notes that the time-dependent observable is a convolution of $P(R)$, the fluctuation-rate distribution, and $1-\exp(-RT_w)$. Convolution with the function $1-\exp(-RT_w)$ will dull any sharp features of $P(R)$ because of the characteristic "width" associated with the convolution. For example, a convolution with a δ-function fluctuation-rate distribution will give an observable that changes over about one order of magnitude in time (see Sec. IV).

Equation (2.15) gives the experimentalist a powerful tool in analyzing the results of a waiting-time-dependent experiment. With this relation, every type of line-narrowing experiment with $T_w > 10\tau$ may be interpreted in a consistent manner yielding the underlying observable—the fluctuation-rate distribution (a somewhat more general treatment can be used for $T_w < 10\tau$). To calculate a fluctuation-rate distribution from experimental data, one convolves a trial function as per Eq. (2.15) and compares it to the data. Thus, experiments with different characteristic time scales, e.g., accumulated echoes[17,28] and time-dependent hole burning,[29] can be analyzed, and the results combined to yield one full fluctuation-rate distribution spanning many orders of magnitude in time—from picoseconds to days or longer.

III. EXPERIMENTAL PROCEDURES

Samples for study consisted of 1.3×10^{-4} M cresyl violet (Exiton) in ethanol, 1.2×10^{-4} M resorufin (Aldrich) in ethanol, and 1.2×10^{-4} M resorufin in glycerol. Lower concentrations of cresyl violet in ethanol were studied as a check. No concentration dependence was observed. The solutions were prepared from fresh stock without further purification with the exception of resorufin in glycerol in which the glycerol was dried over molecular sieves before use.[37] The samples were placed in 1 mm spectroscopic cuvettes and then quickly cooled in a ^{4}He bath cryostat to the temperature of interest. Rapid cooling is necessary to avoid the formation of alternate glassy phases which have been observed when the samples are cooled slowly.[37–39] The samples were held at the low temperature (1.3 or 2.1 K) for 1–2 h before burning any holes to let the samples come to steady state. Effects of sample aging in hole-burning experiments have been reported.[40] Since the waiting time in these experiments was never more than 90 min, 2 h is sufficient to reach steady state on this time scale. Each glass cracked substantially upon formation. Sample quality was the single most important criterion in obtaining good signal-to-noise ratios. Traditional hole-burning experiments could be performed on samples of poorer quality and the data simply averaged. However, due to the sheer magnitude of data and extreme precision required of the results in waiting-time-dependent hole burning, the kind of scatter associated with a poor sample could not be tolerated. All spectra were recorded on the red side of

the O–O absorption, e.g., 620 nm for cresyl violet, 585 nm for resorufin in ethanol, and 587 nm for resorufin in glycerol. The optical densities at these wavelengths and concentrations were as follows: cresyl violet in ethanol, 0.7; resorufin in ethanol, 0.4; and resorufin in glycerol, 0.6.

In the waiting-time-dependent hole-burning experiment, holes were burned with a short laser pulse ($\sim$10–50 ms) and then recorded after various waiting times. (Note that, as a check, holes were also burned and read at a single waiting time. A new spot was used for each single delay. This method gave identical results to burning a single hole and reading it many times after variable delays.) Holes were burned and detected with a Coherent model 599-21 scanning single-mode dye laser (2 MHz bandwidth) under computer control. Burning times and powers are reported in Table I. The laser spot size was fixed at 450 μm radius for each experiment. The burn time and burn power were regulated by two computer-controlled acousto-optic variable-beam attenuators. The laser power could be varied by a factor of up to 5000, and burning pulses as short as a 1–2 ms could easily be produced in this manner. A mechanical shutter blocked the beam when neither burning nor scanning. After burning, a predetermined amount of time was allowed to pass before scanning the hole. The laser was scanned at a rate of $\sim$100 MHz/ms. For waiting times shorter than 20 s only one scan was used to improve time resolution. For times longer than 20 s up to five scans were averaged. In the case of the shortest waiting time (100 ms) there is a small temporal uncertainty since the scan time is on the order of the waiting time. In each experiment, the detection beam was attenuated by a factor of $\sim$2000 relative to the burning beam to minimize the burning effect of the reading beam. With this amount of attenuation, no significant hole shape distortion was observed even after 60 repeated scans.

To span the range of time scales covered in this experiment and still obtain accurate and reproducible results, many modifications were made to the standard hole-burning setup. Second only to sample quality in importance was sample stability. Both short-term vibrations and long-term mechanical drift had to be eliminated before reproducible data could be obtained. In addition, slightly wedged windows ($\sim$1°) were installed on the cryostat to remove the étalon effects associated with parallel windows. Étalon effects should be expected to remain constant in time and, therefore, be easy to normalize out. However, small temperature and mechanical changes over 1000 + s made them unpredictable, requiring their elimination.

Finally, the requirement that data collected with waiting times less than 20 s be recorded with a single scan forced the reduction of all possible sources of noise. The holes were detected in transmission using a cooled photomultiplier tube. A photodiode with a time response matched to that of the phototube was referenced to light from a pickoff placed before the cryostat. Both signals were then divided by an analog divide circuit, and the divided output was then digitized and stored by computer. The fast time (200 ms) holes shown in the figures of Sec. IV are good examples of the signal-to-noise ratios obtained with a single sweep.

TABLE I. Burn times and burn powers used to create spectral holes for various glasses.

Glass	Temperature	Burn time	Burn power	Flux
CV/ETOH	1.30 K	20 ms	12 μW	1900 μW/cm^2
CV/ETOH	2.13 K	50 ms	12 μW	1900 μW/cm^2
Res/ETOH	2.13 K	40 ms	2.5 μW	390 μW/cm^2
Res/ETOH	2.13 K	1.8 s	76 nW	12 μW/cm^2
Res/Gly	2.13 K	16 ms	6.7 μW	1000 μW/cm^2

TABLE II. Burn fluences necessary to obtain a 2% hole after a waiting time of 100 s.

Glass	Temperature	Burn fluence (this work)	Burn fluence (from earlier works)
CV/ETOH	1.30 K	40 μJ/cm^2	31 μJ/cm^2 [a]
CV/ETOH	2.13 K	90 μJ/cm^2	
Res/ETOH	2.13 K	12 μJ/cm^2	9 μJ/cm^2 [b]
Res/Gly	2.13 K	15 μJ/cm^2	11 μJ/cm^2 [b]

[a] From Ref. 43.
[b] From Ref. 22.

Hole depths varied from 1% to 4% depending on burning fluence and waiting time. Table II is a list of burning fluences necessary to obtain a 2% hole after a waiting time of 100 s. Effects which may cause artificial hole broadening, such as sample heating and saturation hole broadening,[41,42] were guarded against in this experiment. The hole depths and hole-burning energies used here are quite comparable to those used in standard hole-burning experiments on the same systems.[22,37,43] The only difference in this study relative to previous ones was the power used to burn the holes. As a check, holes burned with short intense pulses and holes burned with longer (5 s) attenuated pulses were compared after waiting times of 50 to 200 s. In every system with the exception of resorufin in ethanol the results were identical. Therefore, it may be concluded that artificial hole broadening in these systems was not a problem. Resorufin in ethanol proved to be extremely sensitive to burn power, i.e., it was more susceptible to anomalous hole broadening than the other systems. Holes burned with a pulse of 40 ms were universally 0.1 GHz broader than those burned with a longer pulse. The broadening becomes greater when the power is increased and the pulse length shortened. To obtain reasonable data, that is, to burn a 1%–2% hole in a short enough time, a 40 ms burn was used for the data out to $T_w = 10$ s while data taken with $T_w > 10$ s used a burn pulse of 2 s and a proportionally smaller power. When comparing the short- ($T_w \leqslant 10$ s) and long-time data, this 0.1 GHz broadening was taken into account.

The details of the temperature-cycling experiment were identical to that of the standard variable waiting-time experiment with the exception of the temperature control. The sample studied was the identical cresyl violet in ethanol sample used in the fixed-temperature experiment. The hole was burned at 1.3 K and detected after waiting times of 13 and 23 s. The temperature was then ramped to 2.1 K by reducing

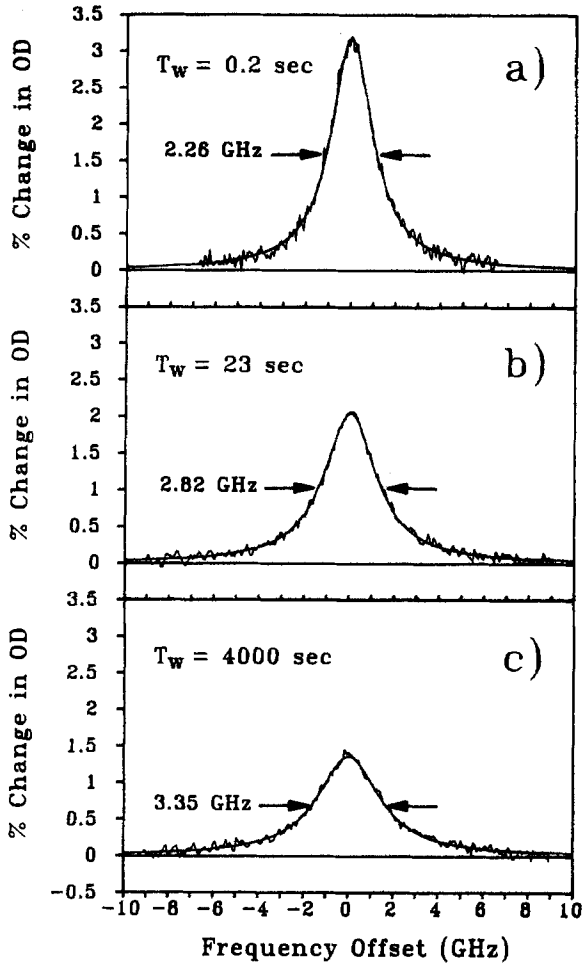

FIG. 1. Three spectra of a hole burned in a 1.3×10^{-4} M cresyl violet in ethanol glass at 1.30 K with various waiting times. The three spectra (a), (b), and (c), were detected with waiting times of 0.2, 23, and 4000 s, respectively. The solid lines are the best Lorentzian fits to the data. The hole was burned at 621 nm for 20 ms with a fluence of 40 μJ/cm^2.

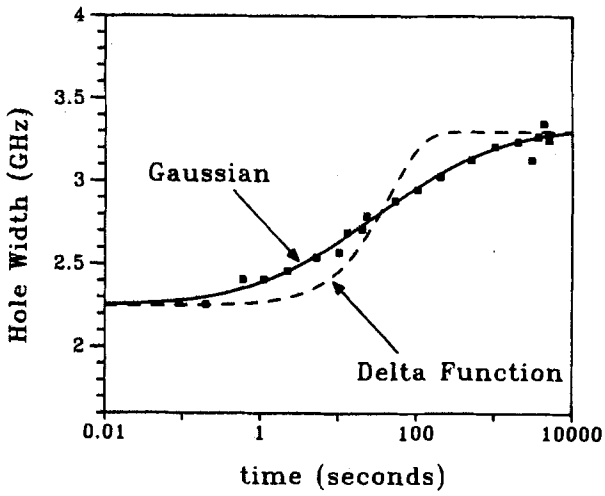

FIG. 2. Semilog plot of the full width at half maximum (FWHM) of various holes vs waiting time for cresyl violet in ethanol at 1.30 K. The hole width broadens most dramatically around 50 s, while flattening out at both short and long times. The solid line through the data is the best fit using log normal distribution of rates [Eq. (4.1)]. See text for values of the parameters. The dashed line is the best fit assuming a δ function distribution of rates, i.e., a single rate. The δ function, while accounting for the magnitude of the broadening, overestimates the steepness of the increase.

the pumping on the liquid helium and bleeding warm helium gas into the cryostat. This process took approximately 50 s to complete. The sample was then held at 2.1 K while the hole was detected at various waiting times. After approximately 500 s, the pump was reopened and the temperature lowered to 1.3 K again. The hole was then recorded again as in the standard waiting-time experiment.

IV. RESULTS AND DISCUSSION

Figure 1 shows a hole burned in the system cresyl violet in ethanol scanned at three different waiting times. The solid line through the data is the best-fit Lorentzian. Note that the holes remain Lorentzian regardless of waiting time. All holes detected in these experiments were Lorentzian regardless of waiting time, depth, burn fluence, and sample. There is no *a priori* reason to expect only Lorentzian holes regardless of experimental parameters. Such a result is indicative of a universal feature of glass dynamics. It has been demonstrated that when the coupling between TLS's and chromophores is dipolar, and the TLS's are uniformly distributed, that the predicted hole shape is Lorentzian regardless of waiting time.[26,31,44,45] This is certainly consistent with these experimental observations.

Figure 2 shows the results of a complete waiting-time-dependent hole-width study for cresyl violet in ethanol at 1.30 K. The hole width is seen to vary over the entire range of study, but the change in width (on a log time scale) is most pronounced in the range of 50 s. Even without the development presented in Sec. II, one could conclude that there exists some process with a characteristic rate around 1/50 s^{-1} in this system. This qualitative information allows one to select a trial form of the fluctuation-rate distribution function. Since convolution with the function $1-\exp(-RT_w)$ according to Eq. (2.15) tends to smooth out any sharp features, there is little point in selecting an excessively complicated form for the fluctuation-rate distribution function. A log normal distribution (Gaussian on a log time scale) was found to be the simplest form which still fits the data. Note that this is by no means a unique solution to the problem of finding $P(R)$. Other functions will also fit the data, for example, a rectangular distribution. However, all functions which fit the data have three features in common—identical center frequencies, identical areas under the curve, and identical characteristic widths. A function which does not contain all of these properties, i.e., a δ function, will not fit the data. A log normal distribution exhibits all properties and is the most physically reasonable. In addition, it fits the data slightly better than unphysical functions such as rectangular distributions. Therefore, it will be used in the analysis of the data.

If the dephasing is due to TLS's and the relaxation of the TLS's is caused by single-phonon scattering, then a log normal distribution of fluctuation rates is equivalent to a Gaussian distribution of tunneling parameters [see Eq. (2.10)].

TABLE III. Parameters which give the best fits to the data for the function $\Delta\omega(T_w) = \Delta\omega_1 + \Delta\omega_2 \int dR\, P(R)[1 - \exp(-RT_w)]$, where $P(R) = (\pi^{1/2}\sigma R)^{-1} \exp\{-[\ln(R/R_0)]^2/\sigma^2\}$.

Glass	Temperature	$\Delta\omega_1$	$\Delta\omega_2$	$\ln(R_0 \cdot 1\,\mathrm{s})$	σ
CV/ETOH	1.30 K	2.25 GHz	1.07 GHz	-3.9 ± 1.0	3.8 ± 1.0
CV/ETOH	2.13 K	4.16 GHz	1.50 GHz	-3.7 ± 1.0	3.8 ± 1.0
Res/ETOH	2.13 K	2.23 GHz	0.89 GHz	-2.9 ± 0.8	4.2 ± 0.8

Such a distribution of tunneling parameters has been used in the analysis of thermodynamic properties, such as time-dependent heat capacities, of amorphous silica.[46] Explicitly, the best fit to the data was achieved when

$$P(R)\,dR \propto \exp\{-[\ln(R/R_0)]^2/\sigma^2\}\,d(\ln R)\,, \quad (4.1)$$

where $\ln(R_0 \cdot 1\,\mathrm{s}) = -3.9 \pm 1.0$ and $\sigma = 3.8 \pm 1.0$ (see Table III for a summary of all fit parameters). The errors listed are obtained by defining $\chi^2 = \Sigma_i \{[y_i - f(i)]/ERRi\}^2$ and including in the limits all fits where $\chi^2 \leqslant \{$No. of data points $-$ No. of free parameters$\}$. The solid line in Fig. 2 is a plot of the best fit using this function. The dashed line in Fig. 2 is an example of the best fit possible when the form of $P(R)$ is assumed to be a δ function, i.e., there is a single rate rather than a broad distribution of rates. One can see that it cannot be made to fit the data nearly as well as the log normal distribution, indicating the underlying fluctuation-rate distribution does have an intrinsic width. Indeed, two δ functions still fail to adequately reproduce the data. When the number is raised to three with freely floating individual rates, the fit becomes better, but is still not as good as the log normal distribution, and there are too many free parameters to achieve a unique fit.

The experiment was repeated at 2.13 K, and these results are plotted along with the 1.30 K results in Fig. 3. A log normal distribution was again used to fit the data at the higher temperature. The best fit (shown as the solid line through the data) was obtained when $\ln(R_0 \cdot 1\,\mathrm{s}) = -3.7 \pm 1.0$ and $\sigma = 3.8 \pm 1.0$. Note that the data indicate that $P(R)$ changes very little with temperature. The center of the distribution remains close to $1/50\ \mathrm{s}^{-1}$. This is consistent with the TLS theory in which the relaxation rate is weakly dependent on temperature [see Eq. (2.10) and accompanying discussion]. Descriptions of glass dynamics other than tunneling TLS tend to predict much more dramatic temperature dependences (see Sec. V). This gives further support to the idea that TLS's are responsible for dephasing in these glassy systems.

Figure 4 is a plot of the fluctuation-rate distribution used to fit the 1.3 K data in Fig. 2. It is produced from a combination of these hole-burning results and previously reported photon-echo data taken on the same sample. The hole-burning results, in addition to yielding Eq. (4.1), give the area under the fluctuation-rate distribution curve for rates faster than the inverse of 10 ms.[29] From the echo data, one may calculate the form of $P(R)$ out to the coherence time of the sample (here ~ 10 ns).[43] It has been shown previously that $P(R) \propto 1/R$ in this region.[43] The $1/R$ distribution when plotted as $P(R) \cdot R$ is a horizontal line. Note that the form of $P(R)$ between 10 ns and 10 ms is unknown. Only

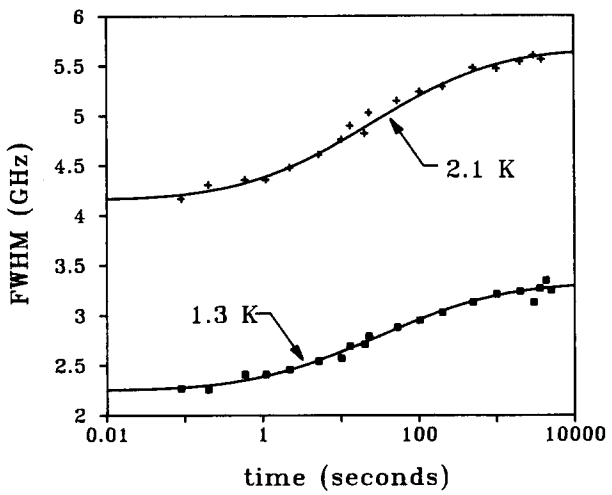

FIG. 3. Plot of hole width vs waiting time for cresyl violet in ethanol at two temperatures, 1.30 and 2.13 K. The solid lines are the best fits assuming a log normal distribution of fluctuation rates. See text for values of the parameters. Examining the curves, one notes that while the magnitude of the broadening increases with temperature, the form does not change, indicating that the distribution of TLS rates is relatively insensitive to temperature.

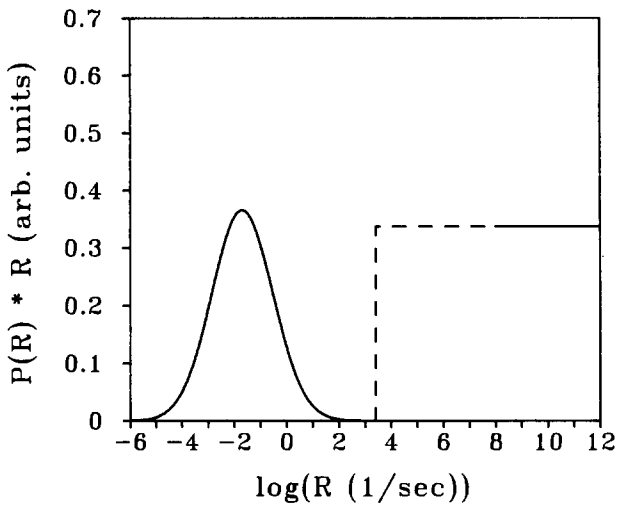

FIG. 4. Plot of the fluctuation-rate distribution, $P(R)$, used to fit the data in Fig. 1. $P(R)$ is a log normal distribution in the region from $R = 100\ \mathrm{s}^{-1}$ to $R = 10^{-5}\ \mathrm{s}^{-1}$ and is flat for $R > 10^8\ \mathrm{s}^{-1}$. The form of the distribution at large R is taken from photon-echo data reported earlier (Ref. 44). The form of the distribution where $10^2 < R < 10^8$ is unclear; however, the area under the curve is known. The dashed line indicates the form the distribution would take assuming it continues flat past $R = 10^8$ until forced to cut off by the area constraint.

the total area under the $P(R)$ curve is known. The dashed line in Fig. 4 is the result which would occur assuming the $1/R$ distribution continues past 10 ns unchanged until forced to cut off by the area constraint. In light of the slow rate results presented here, it is likely that the distribution is more structured than is indicated by the dashed line in Fig. 4. Waiting-time-dependent experiments performed in this region will clarify the nature of the rate distribution.

These time-dependent results are the first to record and analyze the dynamic modes of a glass on this time scale. However, while the results described above quantitatively define the dynamics, they still leave open the question of what is the source of these modes. It has been hypothesized that the dye molecules themselves are responsible for the TLS or, perhaps, are in someway themselves the TLS. If this were the case, the dynamics would be expected to show a marked dependence on the choice of chromophore. To check this, the same type of experiment was carried out on the system resorufin in ethanol at 2.13 K. Figure 5 shows the results of this experiment. The data are reported by subtracting the ~ 0.1 GHz saturation broadening from the short-time data ($T_w \leqslant 10$ s) as was mentioned in Sec. III. The data are presented in this fashion only to give a more accurate description of the actual TLS-induced line broadening. It must be stressed that this adjustment does not affect the relevant results in the calculation of $P(R)$. Fitting the raw data yields exactly the same width and center frequency for the $P(R)$ distribution as a fit to the adjusted data. The fit is simply much better when this broadening is taken into account, and only the magnitude of the broadening is affected.

Examining Fig. 5, one notes that the hole width again broadens in a manner similar to cresyl violet in ethanol—most quickly in the range of $1/50\ s^{-1}$. Fitting the distribution using the form of $P(R)$ in Eq. (4.1) yields the parameters $\ln(R_0 \cdot 1\ s) = -2.9 \pm 0.8$ and $\sigma = 4.2 \pm 0.8$. These values are in agreement with the parameters obtained for the system cresyl violet in ethanol at 2.13 K. In terms of its physical properties, resorufin is dramatically different from cresyl violet. Resorufin's net negative charge should influence its surroundings in a drastically different manner than positively charged cresyl violet. If these dye molecules are themselves the TLS reponsible for glass dynamics, there is little chance that they would yield the identical fluctuation–rate distribution. The fact that the experiments yield the same form for $P(R)$, for the ranges of R's studied, indicates that the dynamic modes are intrinsic to the ethanol glass and are not strongly influenced by the presence of the dye molecule.

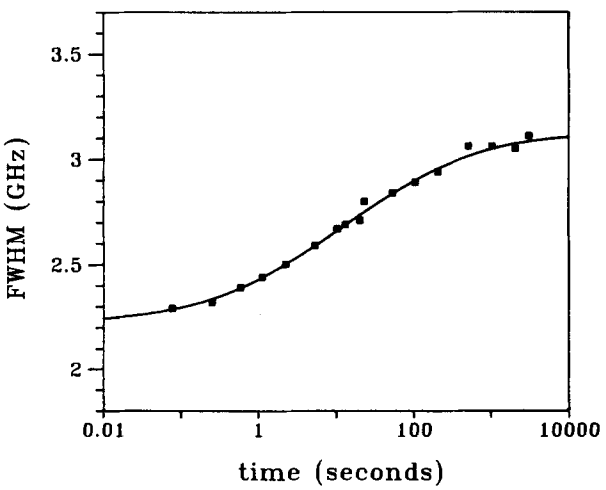

FIG. 5. Plot of FWHM vs waiting time for the system resorufin in ethanol at 2.13 K. The solid line through the data is the best fit using a log normal fluctuation-rate distribution. See text for values of the parameters. The form of the broadening is nearly identical to that of cresyl violet in ethanol, indicating that the dynamics responsible for spectral diffusion on the time scale examined here are intrinsic to the glass and not influenced by the dye molecules.

The $P(R)$ distributions for the two dyes differ in the absolute amount of broadening. This is of no concern, however, since the broadening is directly proportional to the TLS-chromophore coupling strength which is dependent on the choice of dye regardless of the nature of the TLS. In fact, the ratio of the absolute amount of broadening in the two systems is equal to the ratio of the coupling strengths assuming the choice of dye does not severely influence the nature of the glass TLS.[22] The ratio of the amount of broadening from 0.01 to 5000 s in the case of cresyl violet/resorufin in ethanol is 1.7. This is in good agreement with the ratio of the photon-echo linewidths of the two systems which is also equal to the ratio of the coupling strengths—cresyl violet/resorufin two-pulse echo linewidth equals 1.6. This indicates that the coupling strength is basically independent of relaxation rate. While not conclusive, this result is highly suggestive that the coupling mechanism is identical at both short and long times.

By altering the host glass matrix slightly and repeating the previous experiments it should be possible to learn more about the actual nature of the TLS's. To this end, the same type of waiting-time-dependent experiment was performed on cresyl violet in deuterated ethanol—CH_3CH_2OD. The substantially reduced hole-burning efficiency made acquisition of data faster than 2 s difficult; however, the data obtained for waiting times past 2 s were so similar to those obtained in the completely protonated glass as to be indistinguishable to within the scatter of the data. It is evident from this result that motions of the hydrogen bonds alone are not responsible for dephasing for waiting times faster than 10 000 s. This is an interesting result. Hole burning in a totally deuterated mixed ethanol methanol glass seems to have reduced the hole width by over 20%.[21] However, this results was contradicted in a later study which said the results were identical for short waiting times.[47]

Since the dynamics proved to be independent of dye molecule, an experiment was performed on an entirely different glass, resorufin in glycerol. Extensive hole burning and photon-echo results have been reported for this system.[22,37,48] The difference between the linewidths obtained by hole burning and two-pulse photon echoes is only a factor of 3 for this system as opposed to a factor of 8 for cresyl violet in ethanol.[22,37,43] This implies that there is little dynamic activity between the time scales of the two-pulse echo and hole burning. One might expect, therefore, to see little in the way of hole broadening. This is exactly the case. Figure 6 is a

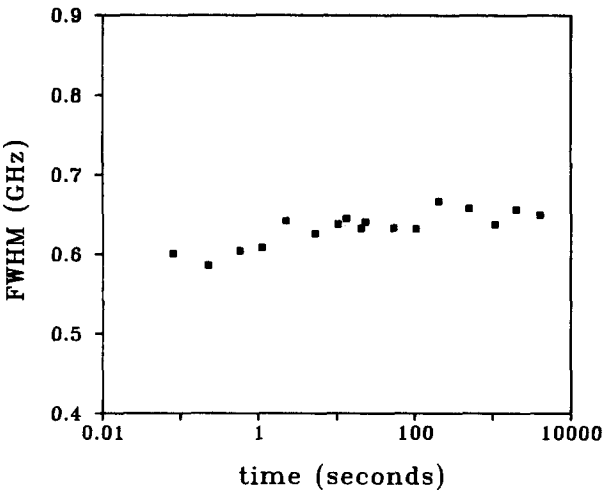

FIG. 6. Plot of the hole width vs log waiting time for the system resorufin in glycerol glass at 2.13 K. There is little apparent hole broadening over the time scale studied here. This confirms that the dynamics observed in ethanol are intrinsic to the ethanol glass. When the glass is changed to glycerol, the hole broadening vanishes.

plot of hole width vs log waiting time for the system resorufin in glycerol. There is essentially no change in hole width over 3 orders of magnitude in time—from 5 s out to 4000 s. There is only the slight suggestion of a change at very fast times ~0.1–5 s. The change is too small to make any predictions about the $P(R)$ distribution at the faster times. However, this results serves as a good counter example to the results obtained in ethanol where a dramatic change was seen, and serves as a further confirmation of the validity of the ethanol measurements. Any phenomena not intrinsic to the glass itself which might be suggested as a source of time-dependent hole broadening should have been observed in the glycerol system just as in the ethanol system.

The absolute magnitude of the hole width in glycerol is different from that reported in previous studies.[48] However, it has been shown that the hole width of resorufin in glycerol is highly dependent upon cooling rate—slower cooling rates yields narrower hole widths.[37] The glycerol sample in this experiment was quickly cooled as is detailed in Sec. III. The hole widths recorded in this experiment agree with those taken on a similarly prepared sample using traditional hole-burning techniques.[37]

The results of the temperature-cycling experiment[49] are detailed in Figs. 7 and 8. Figure 7 shows a single hole detected at 1.30 K before the temperature cycle, after the sample is raised to 2.13 K, and at 1.3 K again after the temperature cycle. The hole broadens when the temperature is raised and narrows again when the temperature is lowered. The time and temperature dependences of the cycled hole width are shown in Fig. 8. The solid lines are the time dependences of the hole width at 1.30 and 2.13 K taken from Fig. 3. The dashed line is a predicted response calculated with no adjustable parameters using the data taken at 1.30 and 2.13 K. The details of the calculation are presented in the next section. The key feature to note is that, after returning to the original temperature, the hole width returns to the value expected without a temperature cycle. That is, the tempera-

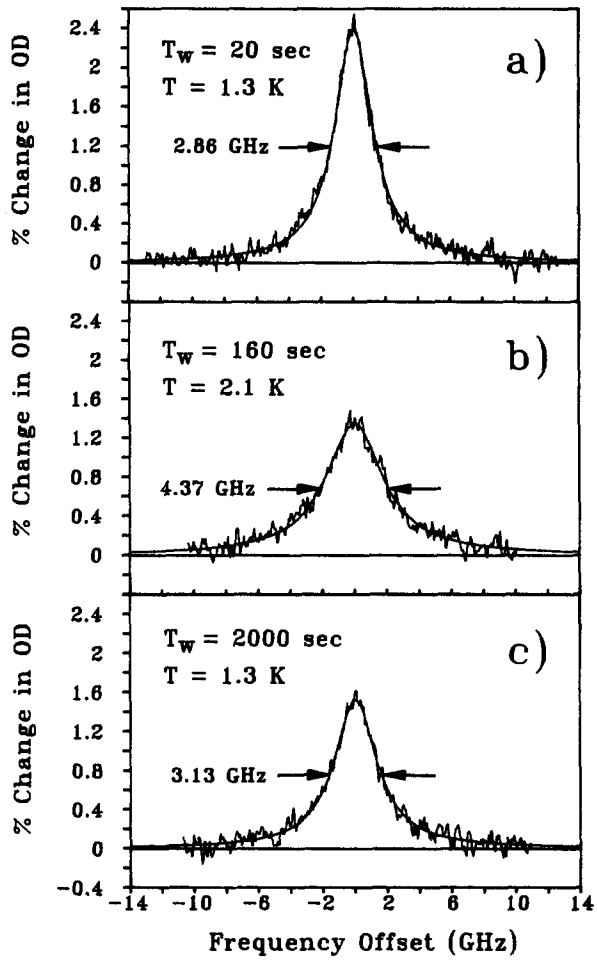

FIG. 7. Three plots demonstrating the effects of temperature cycling on the hole spectra: (a) hole spectrum at 1.3 K and $T_w = 20$ s, before temperature increase; (b) at 2.1 K and $T_w = 160$ s, after temperature increase; and (c) at 1.3 K and $T_w = 2000$ s, after temperature is returned to 1.3 K. The hole broadens when the temperature is raised and returns to its anticipated low-temperature value when the temperature is reduced given the elapsed time.

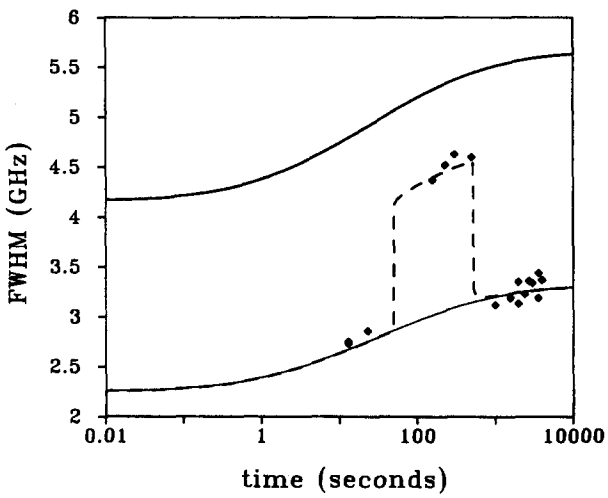

FIG. 8. Plot of the temperature cycled hole width vs waiting time and the comparison with theory. ◆: data recorded from three separate experiments; dashed line: calculation made without adjustable parameters using information obtained from the fits of the data in Fig. 3. Solid lines: (same as those in Fig. 3) show time evolution of holes at the two temperatures without a temperature cycle.

ture-dependent line broadening is totally reversible.

This result indicates, as will be shown in Sec. V, that the glass returns to the same configurational minimum after a temperature cycle as it occupied before the temperature was raised. The fact that this return may be observed on the experimental time scale indicates that the TLS relaxation rate is insensitive to temperature as was also demonstrated in the temperature dependence shown in Fig. 3.

In Sec. V, a theoretical analysis is presented demonstrating the remarkable agreement between the results of the temperature-cycling experiment and the TLS model of glass dynamics. First, however, the problem may be described more qualitatively. Assume the hole is burned at a temperature T_0. According to the TLS model, the TLS with $E \leqslant kT_0$ are constantly fluctuating and, therefore, contribute to hole broadening. The TLS's with $E > kT_0$ are frozen in their ground states. Thus, the width of the hole shortly after burning is only determined by the low-energy TLS. When the temperature is raised to T_1, additional TLS's with $kT_0 \leqslant E \leqslant kT_1$ become active and contribute to hole broadening. When the temperature is returned to T_0, these higher-energy TLS's return to their ground states. The chromophores which make up the hole experience a configuration associated with the higher-energy TLS identical to that experienced when the hole was burned. Thus, the hole width is again determined only by TLS's with $E \leqslant kT_0$, and the sample retains no knowledge that it ever was cycled to a higher temperature.

This model is presented in contrast to a particle or defect diffusion model where the structure of the glass is continually evolving in time. In a diffusive model, raising the temperature would increase the rate of the diffusive motion. When the temperature was again lowered, the diffusive motion would slow again, but continue to randomize the local structure showing no reversible behavior.

An equally accurate description focuses on the motion of the glass configuration upon its potential-energy surface. When the temperature is low, $T = T_0$, the glass configuration may wander upon its N-dimensional potential surface limited only by the restrictions that it cannot access states where $E > kT_0$ or where the transition rate to that state is vanishingly small. This range of motion on the potential surface corresponds to the width of the hole detected at T_0. When the temperature is raised to T_1, the glass may now access different states, i.e., those states where $kT_0 < E < kT_1$. This leads directly to a broader hole at T_1. When the temperature is lowered again, the glass structure returns to those states where $E < kT_0$, and the hole width narrows accordingly. Here it may be seen why it is necessary that the relaxation rate be weakly (linearly or sublinearly) related to temperature. If, at the high temperature, the glass configuration access states which have vanishingly small relaxation rates at T_0, the glass would be frozen in the high-temperature configuration, and the hole width would not narrow again on the time scale of the experiment.

This requirement of weak temperature dependence is satisfied in the TLS model where quantum tunneling is the dominant transition mechanism. If, on the other hand, at the high temperature, thermal hopping begins to appear as the dominant TLS transition mechanism, this would yield an exponential dependence on temperature and an irreversible hole width. Irreversible temperature-cycling hole widths have been reported for many systems.[23–25] However, with the exception of a very few cases,[25] waiting-time dependences have not been taken into account. Indeed, in the system cresyl violet in ethanol one would surmise that the hole width is not completely reversible if one did not take into account the T_w dependence. In addition, there is little irreversibility reported in these systems until the samples are cycled to temperatures of 5–10 K. These temperatures, as the authors suggest, are in the range where the tunneling mode of TLS's begins to break down in favor of a thermal hopping mechanism. When the entire experiment is done in the range where tunneling TLS's dominate and when the T_w dependence is accounted for, the hole width should be reversible as is clearly documented in the next section.

V. THEORY OF TEMPERATURE CYCLE

In this section, the temperature-cycling experiment is analyzed quantitatively as a test of the TLS model. The TLS model has been successful in describing the results of photon-echo and hole-burning measurements in glasses.[1–9] The observed Lorentzian hole shapes and the quasilinear temperature dependence of the hole widths can be derived with the TLS model.[44,45] However, it is possible to explain previous optical experiments using a defect or particle diffusion model, as has been done for heat capacities[19,20] and other experiments on glasses. The reversibility of the temperature-cycled hole widths is a property which cannot be explained with a diffusion-based model. An argument in support of this point based upon the correlation function for a diffusion system is made in Appendix A. In the following discussion the TLS model is used to predict the results of a temperature-cycling study, and the predicted results are compared to the experiment.

The analysis of the temperature-cycling hole burning using the TLS model is identical to that of standard hole burning except in the calculation of the history average. It was implicitly assumed in Sec. II that burning and reading were at the same temperature. When this is not the case, the probability that the TLS has changed state in the time between burning and reading is modified. The form of the history average expressed in Eq. (2.8) is unchanged, i.e.,

$$\langle 1 - \exp(i\phi) \rangle_H = p_{+-}[1 - \exp(2i\Delta\omega\tau)] + p_{-+}[1 - \exp(-2i\Delta\omega\tau)]\,; \quad (5.1)$$

however, the joint probability of finding the TLS in the upper (lower) energy state at $t = 0$ and in the lower (upper) energy state at $t = T_w$ is not as expressed in Eq. (2.7). Equation (2.7) is valid only in the case of constant temperature. Expressed in its most general form, Eq. (2.7) reads

$$p_{+-} = \rho_+(0)\rho_-[T_w|\rho_+(0) = 1]\,,$$
$$p_{-+} = \rho_-(0)\rho_+[T_w|\rho_-(0) = 1]\,, \quad (5.2)$$

where ρ_+ (ρ_-) is the upper (lower) population density of the TLS with respect to its local field, $\rho_-[T_w|\rho_+(0) = 1]$ is again the conditional probability of the TLS being in the lower state at T_w assuming the TLS was in the upper state at $t = 0$. $\rho_+[T_w|\rho_-(0) = 1]$ is defined similarly. Substituting

Eq. (5.2) into Eq. (5.1), one obtains the general result of the history average,

$$\{\rho_+(0)\rho_-[T_w|\rho_+(0)=1] + \rho_-(0)\rho_+[T_w|\rho_-(0)=1]\}\sin^2(\Delta\omega\tau)\,. \quad (5.3)$$

Here we have taken into account that the sign of the coupling $\Delta\omega$ is uncorrelated to the orientation of the local field experienced by the TLS. Therefore, the imaginary parts in Eq. (5.1) cancel.

When the spatial average yields a Lorentzian hole (exponential echo decay), as is usually observed, it is straightforward to show that the width of the hole is given by

$$\Delta\omega_H(T_w) \propto \langle\{\rho_+(0)\rho_-[T_w|\rho_+(0)=1] + \rho_-(0)\rho_+[T_w\rho_-(0)=1]\}\rangle_\lambda\,. \quad (5.4)$$

Thus the entire problem reduces to solving the equation of motion of the TLS.

Take the temperature cycle to be described by a step function, i.e.,

$$T(t) = \begin{cases} T_0, & t \leqslant t_1 \\ T_1, & t_1 \leqslant t \leqslant t_2 \\ T_0, & t > t_2. \end{cases} \quad (5.5)$$

The initial population distributions are $\rho_+(0)=\rho_+(\text{eq};T_0)$ and $\rho_-(0)=\rho_-(\text{eq};T_0)$. The conditional probability $\rho_-[T_w|\rho_+(0)=1]$ for the TLS may then be calculated. To find $\rho_-[T_w|\rho_+(0)=1]$ it is necessary to derive an expression for $\rho_-(T_w)$ for any initial condition. Recalling Eq. (2.6), one has

$$\Delta\rho(t) - \Delta\rho(\text{eq}) = [\Delta\rho(t_0) - \Delta\rho(\text{eq})]\exp[-R(t-t_0)]. \quad (5.6)$$

This can be solved for $\rho_-(t)$. The solution is

$$\rho_-(t) = \tfrac{1}{2}\{1 - \Delta\rho(\text{eq}) + [\Delta\rho(\text{eq}) - \Delta\rho(t_0)] \times\exp[-R(t-t_0)]\}$$
$$= \rho_-(\text{eq}) + [\rho_-(t_0) - \rho_-(\text{eq})]$$

At this point, the temperature-cycling conditions are inserted. During the first interval, $T_w \leqslant t_1$, the conditions are exactly the same as in the fixed-temperature experiment, and the solution is as in Eq. (2.7). During the second and third time intervals the conditional probabilties are found by letting $t_0 = t_1$ and $t_0 = t_2$, respectively. This gives

$$\rho_-[T_w|\rho_+(0)=1]$$

$$= \begin{cases} \rho_-(\text{eq};T_0)\{1-\exp[-R(T_0)T_w]\}\,, & T_w \leqslant t_1 \quad (5.8a) \\ \rho_-(\text{eq};T_1)\{1-\exp[-R(T_1)(T_w-t_1)]\} + \rho_-(t_1)\exp[-R(T_1)(T_w-t_1)]\,, & t_1 \leqslant T_w \leqslant t_2 \quad (5.8b) \\ \rho_-(\text{eq};T_0)\{1-\exp[-R(T_0)(T_w-t_2)]\} + \rho_-(t_2)\exp[-R(T_0)(T_w-t_2)]\,, & T_w > t_2\,. \quad (5.8c) \end{cases}$$

One can show that $\rho_+[T_w|\rho_-(0)=1]$ has the same functional form.

As discussed in Sec. II, for single-phonon-assisted resonant tunneling, the relaxation rate is very weakly dependent on the temperature, $R(T)\sim\coth(E/2kT)$.[8,9,33] Because $R(T)$ is, at most, linear in temperature, the relaxation rates change by much less than a factor of 2 in the temperature range of interest, i.e., 1.3 to 2.1 K. Taking the exact temperature dependence of R into account greatly complicates the problem. Since spectral diffusion takes place on a log time scale, the difference between the predictions of the cycled hole width using the exact form of $R(T)$ and considering $R(T)$ to be constant are imperceptible. That is, the difference is well within the signal-to-noise ratio in this experiment. Therefore, in the temperature range of interest, it can be taken to be independent of T, $R(T_1)=R(T_0)$. This is consistent with our experimental observation (see Sec. IV). Thus, it is easy to see that Eq. (5.8c) becomes identical to Eq. (5.8a) in the long-waiting-time limit, $T_w \gg t_2$. In practice, this condition can always be satisfied in a waiting-time-dependent hole-burning measurement because spectral diffusion broadens the hole on a log time scale. Since Eq. (5.8a) describes the situation where no temperature cycling is present, this indicates that the temperature cycle does not affect the long-time behavior of the hole spectrum.

To calculate the temperature-cycling data, it is necessary to average over all of the TLS's. Following the development in Sec. II, we reduce the average over the internal parameters of the TLS in Eq. (5.4) to an average over the fluxtuation-rate distribution. The details of this conversion are given in Appendix B. The final expression for the time evolution of the hole width including the temperature cycle is

$$\Delta\omega_H(T_w) = \begin{cases} \Delta\omega_0\langle 1-\exp(-RT_w)\rangle_R\,, & T_w \leqslant t_1 \\ A\Delta\omega_0\langle 1-\exp[-R(T_w-t_1)]\rangle_R + \Delta\omega_0\langle\exp[-R(T_w-t_1)] - \exp(-RT_w)\rangle_R\,, & t_1 \leqslant T_w \leqslant t_2 \\ \Delta\omega_0\langle 1-\exp[-R(T_w-t_2)] + \exp[-R(T_w-t)] - \exp(-RT_w)\rangle_R & \\ \quad + A\Delta\omega_0\langle\exp[-R(T_w-t_2)] - \exp[-R(T_w-t_1)]\rangle_R\,, & T_w > t_2\,, \end{cases} \quad (5.9)$$

where A is a scaling constant given by the ratio

$$\langle\rho_+(\text{eq};T_0)\rho_-(\text{eq};T_1) + \rho_-(\text{eq};T_0)\rho_+(\text{eq};T_1)\rangle_E / 2\langle\rho_+(\text{eq};T_0)\rho_-(\text{eq};T_0)\rangle_E\,. \quad (5.10)$$

Here we have taken R to be independent of temperature. The relative population densities at equilibrium in Eq. (5.10) are related to temperature according to $\rho_\pm(\text{eq};T) = [1 + \exp(\pm\beta E)]^{-1}$ where $\beta = 1/kT$. The averages over E in

Eq. (5.10) must be done using the appropriate density of states. It has been shown that, using the TLS model, the density of states of TLS's may be related to the temperature dependence of the hole width in a simple fashion.[22] $P(E) \propto E^{\alpha-1}$ where α is the exponent of the temperature in the temperature dependence, i.e., $\Delta\omega_H(T) \propto T^{\alpha}$. By examining the data in Fig. 3, one can calculate the density of states for the TLS in ethanol. For rates faster than 100 s^{-1}, $P(E) \propto E^{0.2}$. This is consistent with the results of the temperature dependence of the echo decay rate—$T^{1.3\pm0.1}$.[43] For rates slower than 100 s^{-1}, i.e., the log normal distribution, $P(E) \propto E^{-0.3}$.

In Fig. 8, Eq. (5.9) is plotted without adjustable parameters (dashed line) using the information obtained from fitting the standard waiting-time-dependent hole-burning measurements [no temperature cycle (Fig. 3)] at 1.30 and 2.13 K. The temperature-cycling times are $t_1 = 50$ s and $t_2 = 500$ s. The agreement between experiment and the theory based on the TLS model is quite remarkable.

VI. CONCLUDING REMARKS

A combination of careful measurements and theoretical developments are now able to accurately detect and characterize the dynamic modes of complex systems. This allows quantitative information about low-temperature dynamics to be extracted from hole burning or other experimental data. Applying these methods to the organic glass ethanol, it was found that, at low temperatures, there exist modes with a broad distribution of rates. The distribution of rates was characterized for rates which are operative on the 100 ms to 10 000 s time scale. These modes are intrinsic to the glass, i.e., they are independent of dye molecule probe, and they are not related to tunneling of the hydroxyl hydrogen of the ethanol molecule. To date, the exact nature of the modes responsible for spectral diffusion has not been ascertained.

It has been assumed for many years, without conclusive evidence, that the TLS model is an accurate description of low-temperature glass dynamics. The experimental data and the theoretical analysis presented here are the first direct evidence that low-temperature glass dynamics occur on fixed local potential surfaces—a fact completely consistent with the TLS model of glasses and incompatible with other models such as diffusion. The TLS double-well structures should be viewed as an approximate but accurate description of glass potential surface. In fact, the results of temperature-cycling hole-burning measurements agree exactly with the predictions based upon the TLS theory. These results offer overwhelming evidence that the TLS model is an accurate description of the dynamics of low-temperature glasses.

ACKNOWLEDGMENTS

This work was supported by the National Science Foundation Division of Materials Research (No. DMR87-18959). Additional support was provided by the Office of Naval Research (No. N00014-89-J-1119). K.A.L. would like to thank AT&T Bell Laboratories for a Graduate Fellowship.

APPENDIX A

In this appendix it is demonstrated that a diffusion-based model predicts an irreversible hole width. It has been shown that in the limit of slow fluctuations the four-point correlation function for a large number of independent perturbers is[26]

$$C(\tau,T_w,\tau) = \exp\{-N\langle 1-\exp[i\phi(\tau,T_w)]\rangle\},$$
$$\phi(\tau,T_w) = \tau[\Delta\omega(0) - \Delta\omega(T_w)], \quad \text{(A1)}$$

where $\langle\ \rangle$ denotes an average over all the coordinates of the glass, and $\Delta\omega(t)$ is the frequency shift caused by a single perturber. The limit of slow fluctuations implies that $\Delta\omega(t)$ does not vary during the intervals $(0,\tau)$ and $(T_w+\tau, T_w+2\tau)$.

The relevant coordinates in the case of diffusive motion are the initial positions of the perturbers and their relative positions at time T_w. $\Delta\omega(0)$ and $\Delta\omega(T_w)$ may be expressed as functions of these coordinates. $\Delta\omega(0) = \Delta\omega(\mathbf{r})$ and $\Delta\omega(T_w) = \Delta\omega(\mathbf{r}+\mathbf{r}_d)$ where $\mathbf{r}$ is the initial perturber position, and $\mathbf{r}_d$ is the position of the perturber at time T_w relative to its initial location. With this in mind, Eq. (A1) becomes

$$C(\tau,T_w,\tau) = \exp\{-N\langle 1-\exp[i\phi(\mathbf{r},\mathbf{r}_d)]\rangle_{\mathbf{r},\mathbf{r}_d}\},$$
$$\phi(\mathbf{r},\mathbf{r}_d) = \tau[\Delta\omega(\mathbf{r}) - \Delta\omega(\mathbf{r}+\mathbf{r}_d)]. \quad \text{(A2)}$$

If the $\mathbf{r}$ and $\mathbf{r}_d$ distributions have no angular dependence, and the function $\Delta\omega(\mathbf{r})$ is also dependent only upon the magnitude of its argument, the imaginary terms in Eq. (A2) vanish when the averages over $\mathbf{r}$ and $\mathbf{r}_d$ are performed. Thus the correlation function becomes

$$C(\tau,T_w,\tau) = \exp\{-N\langle 1-\cos[\phi(\mathbf{r},\mathbf{r}_d)]\rangle_{\mathbf{r},\mathbf{r}_d}\}$$
$$= \exp\{-2N\langle \sin^2[\phi(\mathbf{r},\mathbf{r}_d)/2]\rangle_{\mathbf{r},\mathbf{r}_d}\},$$

which, when converted to integral form, is

$$C(\tau,T_w,\tau) = \exp\left\{-2N\int \sin^2[\phi(\mathbf{r},\mathbf{r}_d)/2]P(\mathbf{r}) \times P(\mathbf{r}_d,T_w)\,d\mathbf{r}\,d\mathbf{r}_d\right\},$$
$$\phi(\mathbf{r},\mathbf{r}_d) = [\Delta\omega(\mathbf{r}) - \Delta\omega(\mathbf{r}+\mathbf{r}_d)]\,\tau. \quad \text{(A3)}$$

The accumulated phase error, $\phi(\mathbf{r},\mathbf{r}_d)$, is assumed to be monotonically related to $|\mathbf{r}_d|$, that is, $\phi(\mathbf{r},\mathbf{r}_d)$ increases as $|\mathbf{r}_d|$ increases. For the sake of simplicity, the distribution of final perturber positions is assumed to be Gaussian and independent of $\mathbf{r}$. In the simple fixed-temperature case, $P(\mathbf{r}_d,T_w)$ is

$$P(\mathbf{r}_d,T_w) \propto \exp[-r_d^2(4DT_w)^{-1}], \quad \text{(A4)}$$

where D is a diffusion constant. D is a function of temperature and the relevant internal parameters responsible for diffusion. The form of $D(T)$ is unimportant. When the temperature cycle is considered, the form of the $P(\mathbf{r}_d,T_w)$ distribution [Eq. (A4)] is modified. Taking the temperature cycle to be described as a step function, i.e.,

$$T(t) = \begin{cases} T_0, & t \leqslant t_1 \\ T_1, & t_1 \leqslant t \leqslant t_2 \\ T_0, & t > t_2, \end{cases} \quad \text{(A5)}$$

one may show that $P(\mathbf{r}_d, T_w)$ during the temperature cycle is described by

$$P(\mathbf{r}_d, T_w) \propto \begin{cases} \exp[-r_d^2(4D_0T_w)^{-1}], & T_w \leqslant t_1 \\ \exp(-r_d^2\{4[D_0t_1 + D_1(T_w - t_1)]\}^{-1}), & t_1 \leqslant T_w \leqslant t_2 \\ \exp(-r_d^2\{4[D_0t_1 + D_1(t_2 - t_1) + D_0(T_w - t_2)]\}^{-1}), & T_w > t_2, \end{cases} \tag{A6}$$

where D_0 and D_1 are the diffusion constants at the low and high temperatures, respectively. The key feature of Eq. (A6) is that it is a Gaussian of monotonically increasing half width. Recall that the correlation function, Eq. (A3), is directly related to the hole width (rate of decay in an echo experiment).[22,28] By increasing the width of the $P(\mathbf{r}_d, T_w)$ distribution, the averages in Eq. (5.1) are weighted towards larger accumulated phase errors. This leads directly to a faster decaying $C(\tau, T_w, \tau)$ which, when converted to frequency, is equivalent to a broader linewidth. Thus it may be concluded that, in a diffusive model, the linewidth broadens constantly. Cycling the temperature only forces the linewidth to evolve at a different rate at the higher temperature. When the temperature is again lowered, the line does not narrow but merely continues to broaden at the original rate. This is clearly in direct contradiction to the experimental evidence of a reversible linewidth as is documented in Fig. 8. Therefore, it may be concluded that a diffusive model is not valid in these systems.

APPENDIX B

To obtain Eq. (5.9) it is necessary to reduce the average over the TLS internal parameters to an average over the fluctuation-rate distribution. Recall from Eq. (5.4) that

$$\Delta\omega_H(T_w) \propto \langle \{\rho_+(0)\rho_-[T_w|\rho_+(0) = 1] + \rho_-(0)\rho_+[T_w|\rho_-(0) = 1]\}\rangle_\lambda . \tag{B1}$$

For fixed temperature, i.e., $T_w < t_1$, this expression becomes

$$\Delta\omega_H(T_w) \propto \langle 2\rho_-(\mathrm{eq}, T_0)\rho_+(\mathrm{eq}, T_0) \times [1 - \exp(-RT_w)]\rangle_\lambda . \tag{B2}$$

The average over λ is converted to an average R exactly as is done in Sec. II. Thus for $T_w < t_1$ one has

$$\Delta\omega_H(T_w) \propto \langle \langle 2\rho_-(\mathrm{eq}; T_0)\rho_+(\mathrm{eq}; T_0)\rangle_E \times [1 - \exp(-RT_w)]\rangle_R . \tag{B3}$$

Normalizing to the condition that $\Delta\omega_H(T_w > 10\,000\ \mathrm{s}) = \Delta\omega_0$ gives

$$\Delta\omega_H(T_w) = \Delta\omega_0\langle 1 - \exp(-RT_w)\rangle_R . \tag{B4}$$

Examining Eqs. (B3) and (B4), one notes that the constant of proportionality is $\Delta\omega_0/\langle 2\rho_-(\mathrm{eq}, T_0)\rho_+(\mathrm{eq}, T_0)\rangle_E$. This proportionality constant is a temperature-independent term which is related to the TLS–chromophore coupling constant. With this in mind, the hole width at the cycled temperatures may be calculated. Substituting Eq. (5.8b) and the corresponding expression for $\rho_+[T_w|\rho_-(0) = 1]$ into Eq. (B2), the hole width as a function of time in the region $t_1 \leqslant T_w \leqslant t_2$ is obtained. The result is

$$\Delta\omega_H(T_w) \propto \langle 2\rho_-(\mathrm{eq}; T_0)\rho_+(\mathrm{eq}; T_0)[1 - \exp(-Rt_1)]\exp[-R(T_w - t_1)] + [\rho_+(\mathrm{eq}; T_0)\rho_-(\mathrm{eq}; T_1) + \rho_-(\mathrm{eq}; T_0)\rho_+(\mathrm{eq}; T_1)]\{1 - \exp[-R(T_w - t_1)]\}\rangle_\lambda . \tag{B5}$$

This is converted to an average over R as before. Equation (B5) then becomes

$$\Delta\omega_H(T_w) \propto \langle \langle 2\rho_-(\mathrm{eq}; T_0)\rho_+(\mathrm{eq}; T_0)\rangle_E [1 - \exp(-Rt_1)]\exp[-R(T_w - t_1)] + \langle \rho_+(\mathrm{eq}; T_0)\rho_-(\mathrm{eq}; T_1) + \rho_-(\mathrm{eq}; T_0)\rho_+(\mathrm{eq}; T_1)\rangle_E\{1 - \exp[-R(T_w - t_1)]\}\rangle_R . \tag{B6}$$

Substituting the value of the proportionality constant, the final result is obtained for the interval $t_1 \leqslant T_w \leqslant t_2$,

$$\Delta\omega_H(T_w) = \Delta\omega_0\langle \exp[-R(T_w - t_1)] - \exp(-RT_w)\rangle_R + A\Delta\omega_0\langle 1 - \exp[-R(T_w - t_1)]\rangle_R , \tag{B7}$$

where A is a scaling constant equal to

$$\langle \rho_+(\mathrm{eq}; T_0)\rho_-(\mathrm{eq}; T_1) + \rho_-(\mathrm{eq}; T_0)\rho_+(\mathrm{eq}; T_1)\rangle_E / 2\langle \rho_+(\mathrm{eq}; T_0)\rho_-(\mathrm{eq}; T_0)\rangle_E . \tag{B8}$$

The expression for $\Delta\omega_H(T_w)$ when $T_w > t_2$ is evaluated in a similar fashion.

[1] *Amorphous Solids: Low Temperature Properties*, edited by W. A. Phillips (Springer, Berlin, 1981).

[2] *Persistent Spectral Hole Burning: Science and Appliations*, edited by W. E. Moerner (Springer, Berlin, 1988).

[3] J. L. Black and B. I. Halperin, Phys. Rev. B **16**, 2879 (1977).

[4] R. Jankowiak and G. J. Small, Science **237**, 618 (1987).

[5] R. C. Zeller and R. O. Pohl, Phys. Rev. B **4**, 2029 (1971).

[6] R. B. Krumer, R. C. Dynes, and V. Narayanamurti, Phys. Rev. Lett. **40**, 1187 (1978).

[7] M. T. Loponen, R. C. Dynes, V. Narayanamurti, and J. P. Garno, Phys. Rev. Lett. **45**, 457 (1980).

[8] P. W. Anderson, B. I. Halperin, and C. M. Varma, Philos. Mag. **25**, 1 (1972).

[9] W. A. Phillips, J. Low Temp. Phys. **7**, 351 (1972).

[10] B. Golding, J. E. Graebner, B. I. Halperin, and R. J. Schultz, Phys. Rev. Lett. **30**, 223 (1973).

[11] W. Arnold, S. Hunklinger, S. Stein, and K. Dransfeld, J. Non-Cryst. Solids **14**, 192 (1974).

[12] J. Jäckle, L. Piché, W. Arnold, and S. Hunklinger, J. Non-Cryst. Solids **20**, 365 (1978).

[13] B. Golding and J. E. Graebner, Phys. Rev. Lett. **37**, 852 (1976).

[14] C. A. Walsh, M. Berg, L. R. Narasimhan, and M. D. Fayer, J. Chem. Phys. **86**, 77 (1987).

[15] J. Hegarty, M. M. Broer, B. Golding, J. R. Simpson, and J. B. MacChes-

ney, Phys. Rev. Lett. **51**, 2033 (1983); D. L. Huber, M. M. Broer, and B. Golding, *ibid.* **52**, 2281 (1984).
[16]M. M. Broer, B. Golding, W. H . Haemmerle, J. R. Simpson, and D. L. Huber, Phys. Rev. B **33**, 4160 (1986).
[17]L. W. Molenkamp and D. A. Wiersma, J. Chem. Phys. **83**, 1 (1985).
[18]J. M. Hayes, R. Jankowiak, and G. J. Small, in *Persistent Spectral Hole Burning: Science and Applications*, edited by W. E. Moerner (Springer, Berlin, 1988).
[19]C. Yu and A. J. Leggett, Comments Cond. Matter Phys. **14**, 231 (1988).
[20]A. J. Sievers and S. Takeno, Phys. Rev. B **39**, 3374 (1989).
[21]W. Breinl, J. Friedrich, and D. Haarer, J. Chem. Phys. **81**, 3915 (1984).
[22]M. Berg, C. A. Walsh, L. R. Narasimhan, K. A. Littau, and M. D. Fayer, J. Chem. Phys. **88**, 1564 (1988).
[23]J. Friedrich and D. Haarer, Angew. Chem. **23**, 113 (1984).
[24]G. Schulte, W. Grond, D. Haarer, and R. Silby, J. Chem. Phys. **88**, 679 (1988).
[25]W. Köhler, J. Zollfrank, and J. Friedrich, Phys. Rev. B **39**, 5414 (1989).
[26]Y. S. Bai and M. D. Fayer, Phys. Rev. B. **39**, 11 066 (1989).
[27]S. Mukamel and R. F. Loring, J. Opt. Soc. Am. B **3**, 595 (1986); S. Mukamel, Phys. Rev. A **28**, 3480 (1983).
[28]Y. S. Bai and M. D. Fayer, Chem. Phys. **128**, 135 (1988).
[29]K. A. Littau, Y. S. Bai, and M. D. Fayer, Chem. Phys. Lett. **159**, 1 (1989).
[30]R. Kubo, in *Fluctuation, Relaxation, and Resonance in Magnetic Systems*, edited by D. ter Haar (Oliver and Boyd, Edinburgh, 1962).
[31]P. Hu and S. R. Hartmann, Phys. Rev. B **9**, 1 (1974).
[32]P. Hu and L. R. Walker, Phys. Rev. B **18**, 1300 (1978).
[33]B. Golding and J. E. Graebner, in *Amorphous Solids: Low Temperature Properties*, edited by W. A. Phillips (Springer, Berlin, 1981).
[34]D. W. Pack, L. R. Narasimhan, and M. D. Fayer, J. Chem. Phys. (in press).
[35]D. W. Pack and M. D. Fayer, Chem. Phys. Lett. (in press).
[36]J. Bernard and M. Orrit, Chem. Phys. Lett. (submitted); H. Talon, M. Orrit, and J. Bernard, Chem. Phys. (submitted).
[37]K. A. Littau, A. Elschner, and M. D. Fayer, Chem. Phys. Lett. (unpublished).
[38]O. Haida, H. Suga, and S. Seki, J. Chem. Thermochem. **9**, 1113 (1977).
[39]R. van den Berg and S. Völker, Chem. Phys. Lett. **137**, 201 (1987).
[40]J. Miller and J. Friedrich, Chem. Phys. Lett. **134**, 263 (1987).
[41]L. Kador, G. Schulte, and D. Haarer, J. Phys. Chem. **90**, 1264 (1986).
[42]R. van den Berg and S. Völker, Chem. Phys. Lett. **127**, 525 (1986).
[43]L. R. Narasimhan, D. W. Pack, and M. D. Fayer, Chem. Phys. Lett. **152**, 287 (1988).
[44]J. R. Klauder and P. W. Anderson, Phys. Rev. **125**, 912 (1962).
[45]W. B. Mimms, Phys. Rev. **168**, 370 (1968).
[46]R. Jankowiak, G. J. Small, and B. Ries, Chem. Phys. **118**, 223 (1987); R. Jankowiak, J. M. Hayes, and G. J. Small, Phys. Rev. B **38**, 2084 (1988).
[47]W. Breinl, J. Friedrich, and D. Haarer, Phys. Rev. B **34**, 7271 (1986).
[48]R. van den Berg, A. Visser, and S. Völker, Chem. Phys. Lett. **144**, 105 (1988).
[49]Y. S. Bai, K. A. Littau, and M. D. Fayer, Chem. Phys. Lett. **162**, 449 (1989).